OPEN

ORIGINAL ARTICLE

Holographic planar lightwave circuit for on-chip spectroscopy

Giuseppe Calafiore[1,2], Alexander Koshelev[3,4], Scott Dhuey[5], Alexander Goltsov[3], Pavel Sasorov[3], Sergey Babin[1], Vladimir Yankov[3], Stefano Cabrini[5] and Christophe Peroz[1]

Computer-generated planar holograms are a powerful approach for designing planar lightwave circuits with unique properties. Digital planar holograms in particular can encode any optical transfer function with high customizability and is compatible with semiconductor lithography techniques and nanoimprint lithography. Here, we demonstrate that the integration of multiple holograms on a single device increases the overall spectral range of the spectrometer and offsets any performance decrement resulting from miniaturization. The validation of a high-resolution spectrometer-on-chip based on digital planar holograms shows performance comparable with that of a macrospectrometer. While maintaining the total device footprint below 2 cm^2, the newly developed spectrometer achieved a spectral resolution of 0.15 nm in the red and near infrared range, over a 148 nm spectral range and 926 channels. This approach lays the groundwork for future on-chip spectroscopy and lab-on-chip sensing.

INTRODUCTION

Spectrometers are employed in a variety of applications spanning biomedicine to material characterization and product quality control.[1] The core component of spectrometers is a dispersive optical element, such as prisms or diffraction gratings. In conventional spectrometers, light is guided to the dispersive element by a series of mirrors and is ultimately projected onto a detector. These spectrometers can reach ultrahigh resolution and have broad spectral ranges, but their portability and high cost limit their applicability. While the readout electronics can be easily scaled down, the size of spectrometers still represent a bottleneck to the integration with micro/nanoelectromechanical systems[2] or optofluidic devices[3–5] for portable sensing and lab-on-chip capabilities. Thanks to the development of nanophotonic structures to control light at the nanoscale, a number of compact spectrometers have been proposed over the last few years. Although miniaturization of spectrometers was proved to be feasible down to the micrometer scale, performance drops as the device footprint becomes smaller, which generally results in a decrement of resolution or spectral range.[6–9] Integrated spectrometers based on arrayed-waveguide gratings,[10,11] photonic crystals,[12] silicon spiral waveguides,[13] Mach–Zender interferometers,[14] microrings[15] and microresonators[16,17] can reach relatively high resolutions, but their spectral range is narrow and often constrained by the number of output waveguides. Approaches that use planar diffraction gratings[18] and echelle gratings[19,20] are also capable of high resolution, but their working range is mainly limited by their free spectral range.

Conversely, spectrometers based on microelectromechanical systems,[21] filter arrays of Fabry–Perot cavities[22] and particular types of arrayed photonic crystals[23,24] exhibit broad spectral ranges but have a poor resolution. Each of the aforementioned approaches is also not sufficiently resilient to fabrication errors. This problem encouraged the development of a more recent high-resolution spectrometer based on disordered scattering media.[7] Unfortunately, this solution is not flexible and can only work on a narrow spectral range.

To overcome all of these limitations, we have designed and fabricated a novel miniaturized spectrometer based on digital planar holograms (DPHs) that is capable of high resolution over a customizable spectral bandwidth. DPH technology belongs to the class of computer-generated holograms[25] and can encode any specific optical transfer function by manipulating the light in the spectral and spatial domains. In applications like integrated spectroscopy, DPH technology provides several decisive advantages over competing technologies in terms of resolution, bandwidth, robustness to fabrication errors and technology flexibility. As opposed to other approaches where light is dispersed in a continuous spectrum, a DPH spectrometer splits the source light in a discrete number of spectral components and focuses them onto different focal points (Figure 1). We have previously reported the fabrication of the DPH in different waveguide core (SiO_2Ge_x, HfO_2 and Si_3N_4) in order to demultiplex the light in the visible wavelength range.[26–30] Over the years, we have demonstrated that one single planar hologram can reach a high resolution (down to

[1]aBeam Technologies, Hayward, CA 94541, USA; [2]Polytechnic University of Turin, 10129 Turin, Italy; [3]Nano-Optic Devices, Santa Clara, CA 95054, USA; [4]Moscow Institute of Physics and Technology, Moscow 141700, Russia and [5]The Molecular Foundry, Lawrence Berkeley National Laboratory, Berkeley, CA 94720, USA
Correspondence: Dr C Peroz, aBeam Technologies, Castro Valley, CA, USA
E-mail: cp@abeamtech.com
Dr S Cabrini, Lawrence Berkeley National Laboratory, Berkeley, CA, USA
E-mail: scabrini@lbl.gov
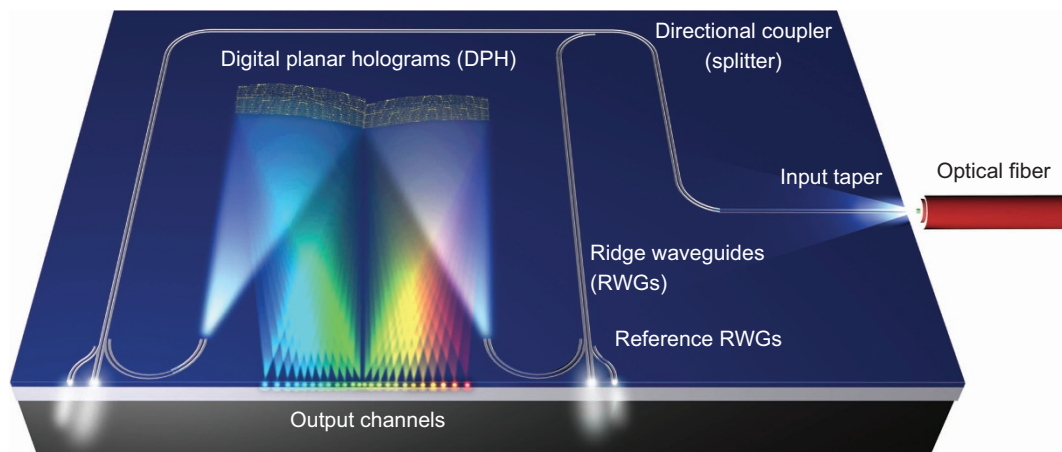Received 23 January 2014; revised 23 May 2014; accepted 26 May 2014

Figure 1 Schematic of an integrated DPH spectrometer. The spectrometer-on-chip integrates one or multiple digital planar holograms and optical circuitry for coupling and wave-splitting operations. The light is brought to the chip with an optical fiber and coupled through a planar taper; light is guided with low losses by ridge waveguides and split based on its bandwidth by directional couplers; once directed to the hologram operating in the relative band, light is demultiplexed and focused on several different output channels at the edge of the chip. DPH, digital planar hologram.

0.015 nm) in a very narrow spectral range[28] (1 nm) or be designed to work over multiple narrow bands[26] (up to 4). Here, we extend these results and demonstrate for the first time that DPHs can be used to build up a high-resolution, broadband spectrometer-on-chip with performance that are similar to conventional spectrometers. Our strategy consists of integrating multiple planar holograms on the same device and connects them with an optical circuitry (Figure 1). Each DPH works in one specific spectral bandwidth, whereas the integrated circuitry includes several functionalities (taper, splitter, waveguide) to efficiently manipulate the light and guide it to the holograms. This geometry overcomes the limitations of devices with one single DPH, and makes it possible to further integrate the optical chip with external optical components, like an input optical fiber and output photodetectors. In this publication, we report the design, the fabrication and the characterization of one photonic device that integrates two DPHs with an optical circuitry, each of them being etched with a different depth in order to maximize their respective efficiency. The spectrometer chip works in two separate spectral bands (630–694 nm and 766–850 nm) for a total spectral bandwidth of 148 nm and 0.15 nm resolution. To the best of our knowledge, this is the first validation of a miniaturized spectrometer with spectral range and resolution that are comparable to conventional spectrometers. This opens a wide range of new opportunities for compact biosensors, lab-on-chip and portable medical diagnostic devices.

MATERIALS AND METHODS

The fundamental idea behind DPH is to exploit the focusing properties of elliptical Bragg gratings[31] and superimpose several elliptical gratings in a miniature supergrating. The supergrating is synthesized by performing a mathematical superposition of the refractive index modulation functions of the multiple sub-gratings, which define the structure. Considering the Fourier components $f_{in}(x,y,\omega)$ and $f_{out}(x,y,\omega)$ of the incoming and outgoing waves propagating through a planar waveguide, it can be shown that to transform $f_{in}(x,y,\omega)$ into $f_{out}(x,y,\omega)$, the variation of the effective refractive index must be computed as $\Delta n_{eff}(x,y) = \int f_{in}(x,y,\omega) f_{out}(x,y,\omega) d\omega$. This equation can also be expressed as $\Delta n_{eff}(x,y) = A(x,y) n_{eff}(x,y)$, where $n_{eff}(x,y)$ is the effective refractive index of the planar waveguide core for the operating propagation mode, transverse electric or transverse magnetic. $A(x,y)$ is

an analog-generating function that describes the modulation of the effective refractive index and delineates the superposition of different interference fringes of diverging and converging light beams. The practical implementation of $A(x,y)$ would imply that the device is fabricated with a multilevel relief and have nanometer resolution, which is impractical and time-consuming with existing lithography techniques. To overcome this complexity, the function $A(x,y)$ is converted into a binary function $B(x,y)$ by using a threshold algorithm to assign 1 s and 0 s. $B(x,y)$ is a spatial map of two-leveled features, corresponding to etched and non-etched areas in the actual fabrication. The algorithm and the device simulations are simplified by replacing curved features of the function $B(x,y)$ with rectangular grooves of the same width. This operation can be regarded as a quantization of the binary function $B(x,y)$. The binarization and quantization of $A(x,y)$ are strongly nonlinear processes that introduce detrimental phenomena like interference between the hologram outputs, scattering to cladding modes or second order core reflections. These problems are minimized by using a specifically developed design code, which dramatically reduces the incoherent scattering. More details about the simulation and design of the DPHs can be found in the Ref. 32.

One of the main properties of DPH technology is its flexibility. Just as computer logic consists of a series of 1 s and 0 s, optical transfer functions associated with any two-dimensional optical device can be generated by the combination of a limited set of holographic symbols defining a two-dimensional diffraction grating. In the specific case of a spectrometer, the DPH would implement a function to demultiplex the input light in the spectral domain, and reflect its components to different focal points (output channels) in the spatial domain. The hologram is embedded into a planar waveguide structure, which consists of a 158-nm-thick silicon nitride film deposited on top of an 8-μm-thick SiO_2 lower cladding on silicon. A high refractive index contrast between the core and the cladding (~25% for Si_3N_4 wafers) further reduces scattering-related propagation losses from the DPH to the cladding modes.

Figure 2a shows a low-magnification optical picture and a scanning electron microscope image of a digital hologram. Light entering the DPHs passes through a gradual variation of the refractive index achieved by lowering the periodicity of the hologram lines on the edge
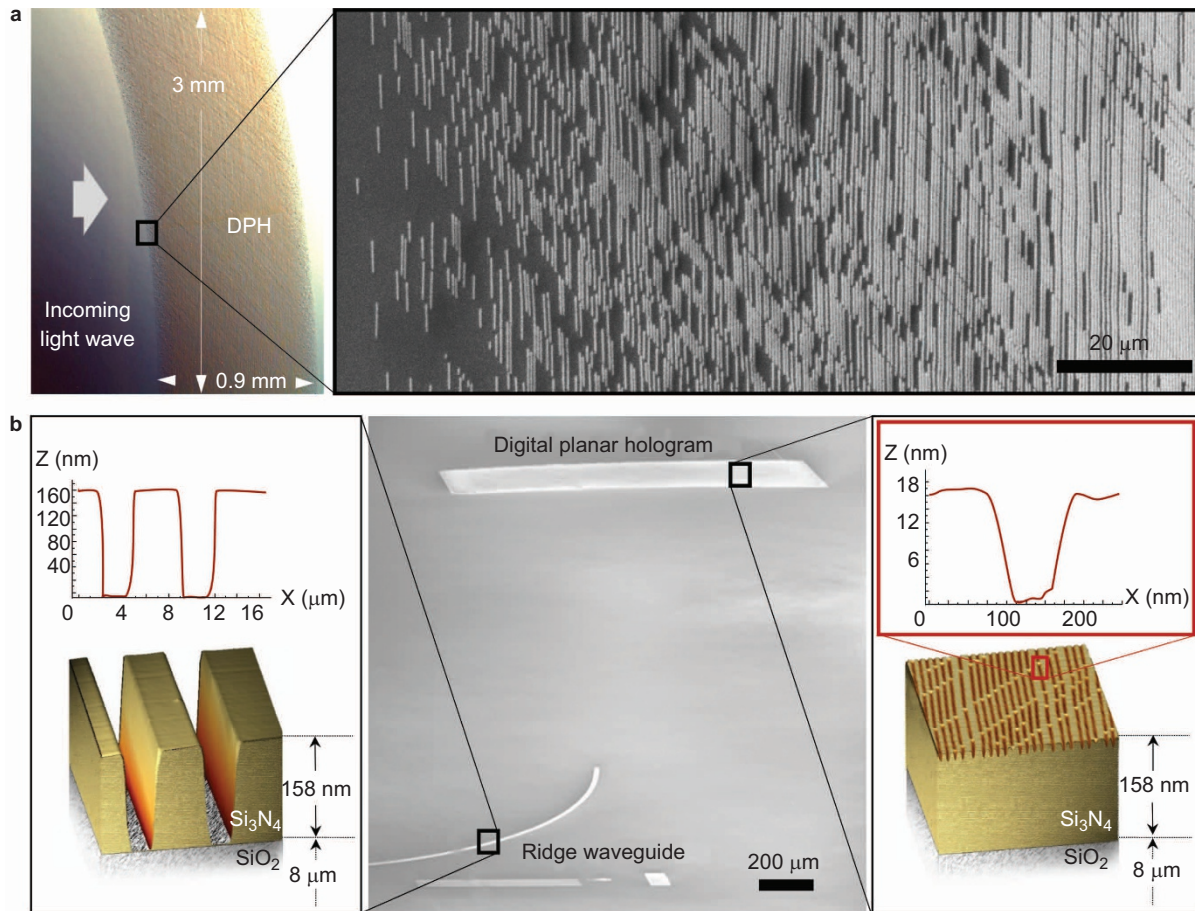
Figure 2 DPH spectrometer fabrication details. (**a**) Light entering the DPH goes through a smooth variation of the refractive index to avoid formation of spurious harmonics; optical microscope photo of the DPH (left), and SEM top-view of a DPH section showing the digitalized grooves embedded into the Si_3N_4 waveguide core (right). (**b**) SEM 30°tilted view of one planar hologram and the projecting RWG (center); the figure shows the atomic force microscopy measurements of the planar hologram, etched 18 nm deep into the waveguide core (right), and the single mode RWG etched through the full Si_3N_4 film (left). DPH, digital planar hologram; RWG, ridge waveguide; SEM, scanning electron microscopy.

(Figure 2a), resulting in the elimination of spurious harmonics[30] that would otherwise be generated. As the light goes through the hologram, it gets reflected according to its wavelength towards different output focal points (channels) spaced 5.25 μm from each other. The depth of the DPHs is kept shallow, typically 10 to 20 nm (Figure 2b), in order to minimize refractive index perturbation and ultimately, increase the spectrometer's resolution. The linewidth of the DPH grooves is fixed to be $\lambda_c/4n_{eff}$, λ_c being the central wavelength of the DPH. Each hologram is optimized to reach high performance on one spectral band of about 100 nm. Thus, in order to build broadband and/or multiple-band spectrometer-on-chips, we have developed a specific type of optical architecture that couples several single-band DPHs in parallel on the same chip (Figure 1). The solution that we designed consists of an optical circuit that connects the entire device and expands its functionalities. Light is introduced from a single mode fiber to the chip by means of a taper[33] to reduce coupling losses by matching the mode profiles in the horizontal direction. The input light is then split by directional couplers[34,35] according to its spectral band (Figure 3) and directed through two distinct ridge waveguides (RWGs) to the two holograms, which are working in the separate spectral bands 630–694 nm (436 channels) and 766–850 nm (490 channels) respectively for a total bandwidth of 148 nm and 0.15 nm spectral resolution. Figure 3a and 3b shows the response of the splitter in case of

$\lambda=662$ nm and $\lambda=805$ nm, respectively. At these wavelengths, the splitting ratio is maximum and the light is fully directed to the correspondent DPH. The dashed area in Figure 3c indicates the light that is sent to the opposite DPH, when the splitting efficiency is not maximum. Part of this light is transmitted through the hologram, the remaining part is dispersed upwards to the upper cladding, and consequently does not contribute to the output channel intensities since it is not reflected by the hologram that receives it. All of the optical elements that belong to the circuitry are optimized for the highest efficiency in the visible light range, and, unlike the DPHs, are etched through the full thickness of the waveguide core to reach a higher confinement of the light and reduce the losses in tight turns (Figure 2b).

The substrate consists of Si/SiO_2 (8 μm)/Si_3N_4 (158 nm), from Lionix BV.[36] The planar holograms and the optical circuitry are fabricated by a twofold electron beam lithography (EBL) and reactive ion etching process, over two successive steps, for the optical circuitry and the holograms, respectively. Direct EBL writing is performed at 100 kV and 500 pA using a Vistec VB-300 EBL system. ZEP 520A is the resist used for the lithography with variable thickness: 200 nm and 60 nm for the optical circuitry and the DPHs, respectively. This is covered by a 100 nm thick conductive polymer, Aquasave ZA. This process is carefully reported in Ref. 37. Specific EBL proximity corrections are applied
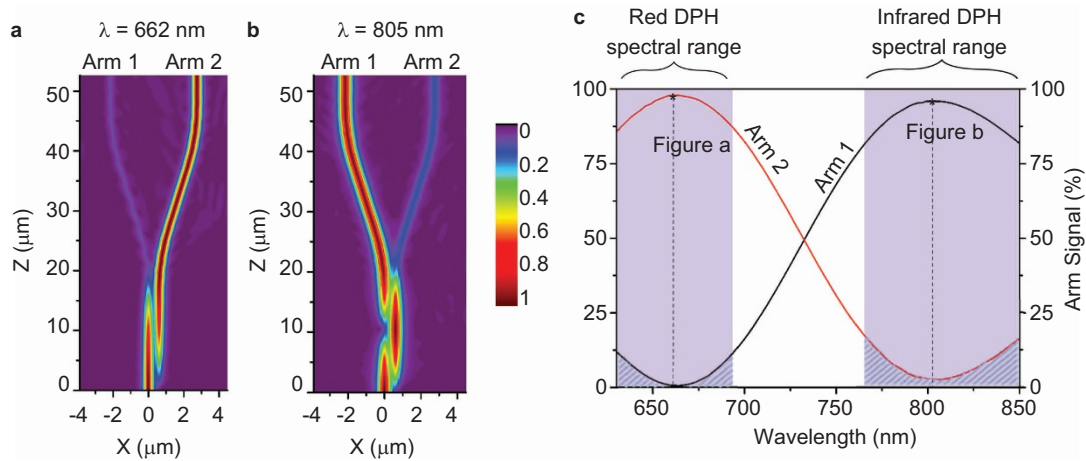
Figure 3 Simulation of integrated light splitter. Optical responses of one directional light coupler for an input wavelength of (**a**) 662 nm and (**b**) 805 nm. The light that enters the splitter is guided to different waveguides according to its wavelength. This device is used to bring light to different DPHs and is the main component that allows the integration of multiple holograms and consequent spectral broadening. (**c**) The splitting efficiency is mapped in function of the wavelength. For some wavelengths, the part of the light is guided to the opposite DPH. Note that this light would not compromise the device performance as it is not reflected back to the output channels. It is dispersed upwards to the cladding by the DPH and transmitted through it. DPH, digital planar hologram.

with CATS software from Synopsis.[38] Plasma etching processes are carried out with a Reactive Ion Etching tool (Oxford Plasmalab 80) and optimized for slow etching, high vertical sidewalls and minimum edge roughness. The optical circuitry is etched through the full thickness of the waveguide core with a mixture of 50 sccm CHF_3–4% O_2 at 55 mT of pressure and 50 W of radio frequency power. The same recipe is used for etching the DPH grooves with power reduced to 25 W to have more precise control over the etching depth. The planar structure of DPHs makes them compatible with high-volume manufacturing by standard complementary metal oxide semiconductor lithography techniques and nanoimprint lithography, as shown in our previous work.[39] After the lithography step, the chip is covered with a 2-μm-thick SiO_2 upper cladding that is deposited by plasma enhanced chemical vapor deposition at 350 °C to protect the DPH structure and minimize light scattering.[27]

RESULTS AND DISCUSSION
The holographic spectrometers were tested using the optical set-up described in detail in Ref. 27. A micro-objective system is used to

project the demagnified image of the output fiber from the light source to the input of the DPH chip. In experiments an optical parametric oscillator with a 0.2-nm-bandwidth that is tunable in the range of 400–2700 nm is used, unless otherwise specified. The power and spectrum of light at the DPH input is monitored with the Avantes-2048 spectrometer,[40] which has a spectral resolution of 0.4 nm. Simulations of the light propagation and reflection into the planar hologram are performed with the proprietary code Spectroplan.[41] The upper section of the Figure 4 maps the simulated geometrical distribution of the hologram's reflectivity for the DPH that operates in the red wavelength range, when it is illuminated at $\lambda=660.59$ nm. Simulations show that the reflectivity of the hologram in one output channel is around 35%±5%. To determine the actual reflective power of our holograms, a second directional coupler, that is located in proximity of the RWG end, splits the light with a splitting ratio of 10%. The main portion of light is directed towards the hologram *via* a single-mode RWG, while the rest is coupled into a reference RWG (Figure 1). By comparing the signals at the reference RWGs to the output of the hologram, the actual coupling efficiency of the splitters and reflectivity
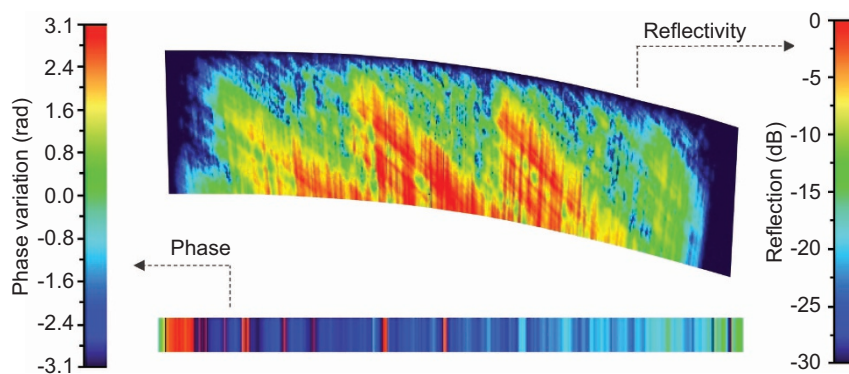

Figure 4 Simulation of the response of the red-spectrum operating DPH to a 660.59 nm laser: reflectivity and phase. It shows the distribution of the intensity (top) and phase (bottom) of the light reflected into channel 218, which corresponds to the laser wavelength of 660.59 nm. The reflectivity profile allows the light to converge cylindrically into the output channel, which is located at a fixed distance on the edge of the chip. The optical path from the DPH to the channel varies from one side of the hologram to the other. To account for the difference in path and have coherent interference of beams that converge into the same output focal point, phase of the reflected light must be set accordingly. DPH, digital planar hologram.

of the holograms can be calculated. In good agreement with our simulations, the reflection of the DPHs was evaluated to be 40%±15%, depending on several parameters, including hologram depth. The value of reflection is calculated, accounting for material losses along free space propagation, which were measured to be around 2 dB cm^{-1} for wavelengths in the range of 600–900 nm. The losses associated with the vertical edge roughness of the RWGs are found to be around 6 dB m^{-1} (at 660 nm wavelength) due to the high field amplitude at the edge of the waveguides. These losses are reduced by adiabatically widening the RWG linewidths up to 5 μm over long straight paths.[42,43] The total output/input ratio is around −15 dB, mostly due to material losses and the low coupling efficiency measured to be around 20% for wavelengths from 600 to 800 nm. The stray light due to imperfect coupling of the fiber with the input RWG is visible in Figure 5a. In spite of these losses, an input spectral intensity as low as 50 pw nm^{-1} is sufficient for signal detection (3σ level) with an integration time of 10 ms.

The lower section of Figure 4 shows the simulated variation of the beam phases at the output of the hologram. The phases that light beams with the same wavelength acquire when reflected by the DPH

are assigned accounting for the different optical paths from the DPH to the output channel. With the correct phase shift, light will constructively interfere at the focal points, maximizing the output intensities. A representation of the output light profile and output intensities is shown in Figures 5b. The intensity distribution at the output plane of the DPH is recorded using a charge-coupled device camera (50 frames per second).

The physical position of the activated output channel is univocally determined by the wavelength of the input light. Figure 5b illustrates the intensity profile of the output channels when a laser beam with 10 pm bandwidth illuminates the device input; as expected, only one channel is activated. By comparing adjacent channel intensities (Figure 5c), the device cross-talk can be measured. The cross-talk is defined as the ratio between the light intensity in one channel and the intensity of the interfering light in lateral channels. In our spectrometer, it is evaluated to be around 10 dB over the entire spectral range, which is adequate to allow the analysis of complex spectra. Figure 5c shows the response to six different wavelengths and the relative correspondence to the output channel number. Reporting wavelengths to wavenumbers, their association with relative channel numbers is
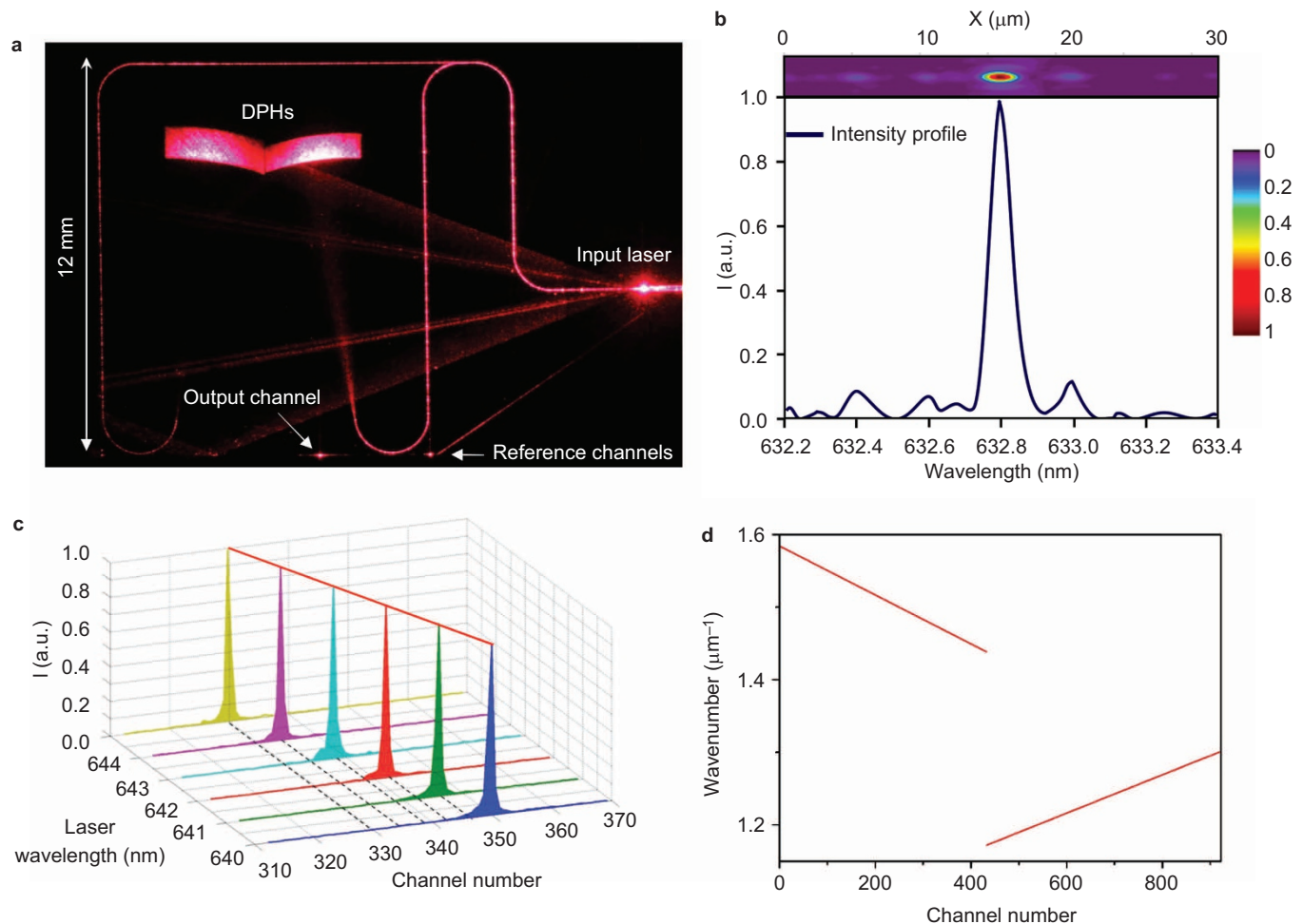

Figure 5 Optical responses of a 926 channel spectrometer. (**a**) Optical top-view photo of a chip illuminated at the input by a HeNe laser with an emission peak at 632.8 nm and a 10 pm FWHM bandwidth, TE polarization. The visible light rays coming out of the input edge (stray light) are due to a non-ideal matching between the modal size of the macroscopic optical fiber and the microscopic RWG. (**b**) Profile of the normalized light intensity at the spectrometer output; on the top, output light detected by photodetectors from the chip edge. (**c**) Response of the device to six different wavelengths and their relative correspondence to different channel numbers. (**d**) Linearity of the dispersion curve of the two-hologram spectrometer. The shape of the dispersion curve can by customized be design to assume any profile. FWHM, full-width at half-maximum; RWG, ridge waveguide; TE, transverse electric.

plotted in Figure 5d, which shows the linearity of the device dispersion curve with accuracy better than 20% of channel spacing, as expected by design. In addition to the bandwidth and resolution, the dispersion curve of a DPH spectrometer can be customized to assume any specific profile, allowing resolution changes over different bands of interest for specific applications. Initial attempts to integrate the spectrometer with an electronic readout were performed. A temperature monitor of the DPH-detector assembly was provided in the integration. As a result, after the proper temperature–wavelength calibration, the device showed strong resistance to temperature variation and enabled the identification of isolated narrow laser lines with an accuracy of about 20 pm.

The spectral emission of a laser diode was measured by our spectrometer and compared with the response from a standard spectrometer that is commercially available (Figure 6). The edge view of the light coming out of the channels is taken by a charge-coupled device array and reported in Figure 6 (upper section; the gray profile plots the actual channel light intensities). Light between the maxima of the grey curve in Figure 6 is concentrated into the nearby peaks. The spline interpolation of this 'quantized' reading constitutes the spectrum of the incoming light (in green) as seen by our spectrometer, while the red curve is the spectrum of the same laser diode measured by the Avantes spectrometer. Both spectrometers present similar optical responses. This result validates DPH technology as a competitive candidate to the development of on-chip spectroscopy, and opens a wide range of unexplored opportunities for lab-on-chip development.
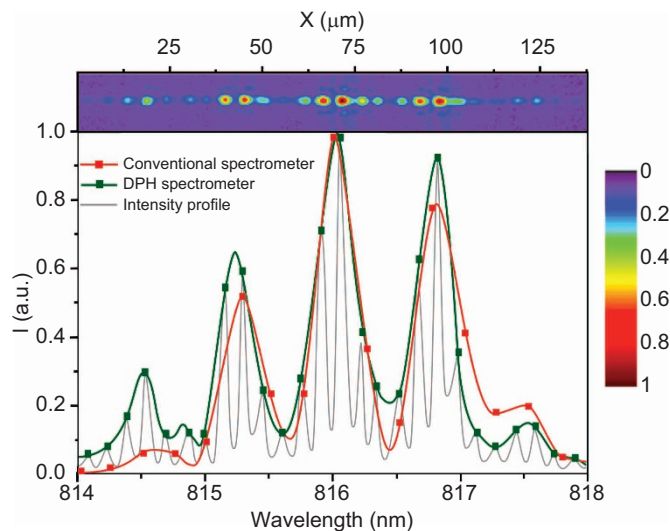

Figure 6 Validation of the DPH technology for making spectrometer-on-chip. Comparison between the optical responses to a laser diode input light beam of a DPH spectrometer-on-chip (green) and a commercial conventional spectrometer (red). The gray line represents the actual profile of the light exiting the 26 output channels spread over the 137.5 μm DPH chip edge. Meaningful information of the input spectrum can be determined by interpolation of the channel peaks. A third-order spline is used to outline the DPH spectrum, reported in green. The resolution of the DPH spectrometer used in this experiment is 0.15 nm/channel whereas the other spectrometer has 0.4 nm resolution. Light emitted by the laser diode is split and sent to the compact and conventional spectrometers for analysis; responses are then overlapped and compared. From the similarity of the two curves, we can conclude that performances of DPH spectrometer-on-chip can compete with that of a traditional spectrometer (within the reading tollerance of the two devices). DPH, digital planar hologram.

CONCLUSIONS

We have reported a novel solution to integrate multiple digital planar holograms on the same chip and demonstrated the first spectrometer-on-chip that presents performance that is competitive with conventional macro-spectrometers. While the area occupied by a DPH is below 3 mm^2 and the overall device footprint is smaller than 2 cm^2, the spectrometer has a resolution as low as 0.15 nm over 148 nm spectral range and 926 channels. Integration of multiple DPHs based on the ideas reported here promises development of an even broaderband compact spectrometer. The sensitivity, resolution, dispersion curve and spectral region of spectrometers can be easily customized exploiting the flexibility of our DPH design code to cover a large wavelength range, from visible light to mid-wavelength infrared, and can be produced at a low cost by nanoimprint lithography. The already small footprint can be further reduced by monolithically integrating photodetectors on chip, in order to shorten the distance between the output plane and the holograms, and minimize the required volume. We believe that DPH technology offers a unique platform for developing a miniaturized, broadband, high resolution and on-demand spectrometer for a new variety of lab-on-chip applications and sensors.

1   Savage N. Spectrometers. *Nat Photonics* 2009; **3**: 601–602.
2   Song W, Liu A, Lim C, Yap P. A micro-optic-fluidic spectrometer with integrated 3 liquid-liquid waveguide. In Proceedings of 2007 IEEE/LEOS International Conference on Optical MEMS and Nanophotonics; 12–16 August 2007; Hualien, Taiwan. IEEE: New York, USA, 2007, pp161–162.
3   Hu Z, Glidle A, Ironside CN, Sorel M, Strain MJ *et al*. Integrated microspectrometer for fluorescence based analysis in a microfluidic format. *Lab Chip* 2012; **12**: 2850–2857.
4   Schmidt O, Bassler M, Kiesel P, Knollenberg C, Johnson N. Fluorescence spectrometer-on-a-fluidic-chip. *Lab Chip* 2007; **7**: 626–629.
5   Gallegos D, Long KD, Yu H, Clark PP, Lin Y *et al*. Label-free biodetection using a smartphone. *Lab Chip* 2013; **13**: 2124–2132.
6   Wolffenbuttel RF. State-of-the-art in integrated optical microspectrometers. *IEEE Trans Instrum Meas* 2004; **53**: 197–202.
7   Redding B, Liew SF, Sarma R, Cao H. Compact spectrometer based on a disordered photonic chip. *Nat Photonics* 2013; **7**: 746–751.
8   Jovanov V, Ivanchev J, Knipp D. Standing wave spectrometer. *Opt Express* 2010; **18**: 426–438.
9   Avrutsky I, Chaganti K, Salakhutdinov I, Auner G. Concept of a miniature optical spectrometer using integrated optical and micro-optical components. *Appl Opt* 2006; **45**: 7811–7817.
10 Cheben P, Schmid JH, Delâge A, Densmore A, Janz S *et al*. A high-resolution silicon-on-insulator arrayed waveguide grating microspectrometer with sub-micrometer aperture waveguides. *Opt Express* 2007; **15**: 2299–2306.
11 Barbarin Y, Leijtens XJ, Bente EA, Louzao CM, Kooiman JR *et al*. Extremely small AWG demultiplexer fabricated on InP by using a double-etch process. *IEEE Photonics Technol Lett* 2004; **16**: 2478–2480.
12 Momeni B, Hosseini ES, Askari M, Soltani M, Adibi A. Integrated photonic crystal spectrometers for sensing applications. *Opt Commun* 2009; **282**: 3168–3171.
13 Velasco AV, Cheben P, Bock PJ, Delâge A, Schmid JH *et al*. High-resolution Fourier-transform spectrometer chip with microphotonic silicon spiral waveguides. *Opt Lett* 2013; **38**: 706–708.
14 Florjańczyk M, Cheben P, Janz S, Scott A, Solheim B *et al*. Multiaperture planar waveguide spectrometer formed by arrayed Mach–Zehnder interferometers. *Opt Express* 2007; **15**: 18176–18189.
15 Nitkowski A, Chen L, Lipson M. Cavity-enhanced on-chip absorption spectroscopy using microring resonators. *Opt Express* 2008; **16**: 11930–11936.

16 Xia Z, Eftekhar AA, Soltani M, Momeni B, Li Q *et al*. High resolution on-chip spectroscopy based on miniaturized microdonut resonators. *Opt Express* 2011; **19**: 12356–12364.

17 Sweeney SJ, Zhang Y, Goodyer ID. The development of a novel monolithic spectrometer chip concept. *Proc SPIE* 2012; **8264**: 82640O.

18 Kyotoku BB, Chen L, Lipson M. Sub-nm resolution cavity enhanced microspectrometer. *Opt Express* 2010; **18**: 102–107.

19 Keliher PN, Wohlers CC. Echelle grating spectrometers in analytical spectrometry. *Anal Chem* 1976; **48**: 333A–340A.

20 Ma X, Li M, He J. CMOS-compatible integrated spectrometer based on echelle diffraction grating and MSM photodetector array. *IEEE Photonics J* 2013; **5**: 6600807.

21 Khalil D, Omran H, Medhat M, Saadany B. Miniaturized tunable integrated Mach–Zehnder MEMS interferometer for spectrometer applications. *Proc SPIE* 2010; **7594**: 75940T.

22 Correia J, Bartek M, Wolffenbuttel R. Bulk-micromachined tunable Fabry–Perot microinterferometer for the visible spectral range. *Sens Actuators A Phys* 1999; **76**: 191–196.

23 Xu Z, Wang Z, Sullivan ME, Brady DJ, Foulger SH *et al*. Multimodal multiplex spectroscopy using photonic crystals. *Opt Express* 2003; **11**: 2126–2133.

24 Pervez NK, Cheng W, Jia Z, Cox MP, Edrees HM *et al*. Photonic crystal spectrometer. *Opt Express* 2010; **18**: 8277–8285.

25 Hariharan P. *Optical Holography: Principles, Techniques and Applications*. Vol. 20. Cambridge: Cambridge University Press; 1996.

26 Peroz C, Calo C, Goltsov A, Dhuey S, Koshelev A *et al*. Multiband wavelength demultiplexer based on digital planar holography for on-chip spectroscopy applications. *Opt Lett* 2012; **37**: 695–697.

27 Calò C, Lacatena V, Dhuey S, Cabrini S, Babin S *et al*. Fabrication of digital planar holograms into high refractive index waveguide core for spectroscopy-on-chip applications. *J Vac Sci Technol B Microelectron Nanometer Struct* 2012; **30**: 06FE01.

28 Babin S, Bugrov A, Cabrini S, Dhuey S, Goltsov A *et al*. Digital optical spectrometer-on-chip. *Appl Phys Lett* 2009; **95**: 041105.

29 Yankov V, Babin S, Ivonin I, Goltsov A, Morozov A *et al*. Multiwavelength Bragg gratings and their application to optical MUX/DEMUX devices. *IEEE Photonics Technol Lett* 2003; **15**: 410–412.

30 Peroz C, Goltsov A, Dhuey S, Sasorov P, Harteneck B *et al*. High-resolution spectrometer-on-chip based on digital planar holography. *IEEE Photonics J* 2011; **3**: 888.

31 Henry CH, Kazarinov RF, Shani Y, Kistler RC, Pol V *et al*. Four-channel wavelength division multiplexers and bandpass filters based on elliptical Bragg reflectors. *J Lightwave Technol* 1990; **8**: 748–755.

32 Yankov V. Method of digitally processing optical waves and an integrated planar optical device based on digital planar holography. US Patent 20090190195 A1. 2009 Jul 30.

33 Felici T, Engl H. On shape optimization of optical waveguides using inverse problem techniques. *Inverse Probl* 2001; **17**: 1141–1162.

34 Ghatak A, Thyagarajan K, Thyagarajan K. *An introduction to Fiber Optics*. Cambridge: Cambridge University Press; 1998. p373–375.

35 Lee CW, Darmawan S, Lee SY, Chin MK. Design of polarization-independent wavelength splitter based on single directional coupler. In: *Integrated Photonics Research and Applications*. San Diego, California, April 10, 2005. ISBN: 1-55752-787-3. OSA society.

36 LionixBV. http://www.lionixbv.com.

37 Babin S, Peroz C, Bugrov A, Goltsov A, Ivonin I *et al*. Fabrication of novel digital optical spectrometer on chip. *J Vac Sci Technol B Microelectron Nanometer Struct* 2009; **27**: 3187–3191.

38 Synopsys. http://www.synopsys.com.

39 Peroz C, Dhuey S, Goltsov A, Vogler M, Harteneck B *et al*. Digital spectrometer-on-chip fabricated by step and repeat nanoimprint lithography on pre-spin coated films. *Microelectron Eng* 2011; **88**: 2092–2095.

40 Avantes. http://www.avantes.com

41 Svetikov V, Peroz C, Ivonin I, Dhuey S, Cabrini S *et al*. Suppression of lateral modes in wide aperture laser diodes by digital planar holograms. *Proc SPIE* 2011; **7918**: 79180P.

42 Specto S, Geis MW, Lennon D, Williamson RC, Lyszczarz TM. Hybrid multi-mode/single-mode waveguides for low loss. In: *Integrated Photonics Research*. San Francisco, California June 30, 2004. ISBN: 1-55752-774-1. OSA society.

43 Chin MK, Lee CW, Lee SY, Darmawan S. High-index-contrast waveguides and devices. *Appl Opt* 2005; **44**: 3077–3086.